# Supporting Information

# for

# Synthesis and in vitro biochemical evaluation of oxime bond linked daunorubicin–GnRH-III conjugates developed for targeted drug delivery

Sabine Schuster[1,2], Beáta Biri-Kovács[1,2], Bálint Szeder[3], Viktor Farkas[4], László Buday[3], Zsuzsanna Szabó[5], Gábor Halmos[5] and Gábor Mező[1,2]*

Address: [1]MTA-ELTE Research Group of Peptide Chemistry, Hungarian Academy of Sciences, Eötvös L. University, 1117 Budapest, Hungary, [2]Institute of Chemistry, Eötvös L. University, 1117 Budapest, Hungary, [3]Research Centre for Natural Sciences, Institute of Enzymology, Hungarian Academy of Sciences, 1117 Budapest, Hungary, [4]MTA-ELTE Protein Modelling Research Group, Hungarian Academy of Sciences, Eötvös L. University, 1117 Budapest, Hungary and [5]Department of Biopharmacy, Faculty of Pharmacy, University of Debrecen, 4032 Debrecen, Hungary

Email: Gábor Mező - gmezo@elte.hu

*Corresponding author

## Characterization data for compounds 1–6: RP-HPLC chromatograms and ESI–MS spectra; fragments of 1–6 produced by lysosomal rat liver homogenate; cellular uptake of K1, K2, 1, 2, 4, 5 by CLSM

## Table of contents

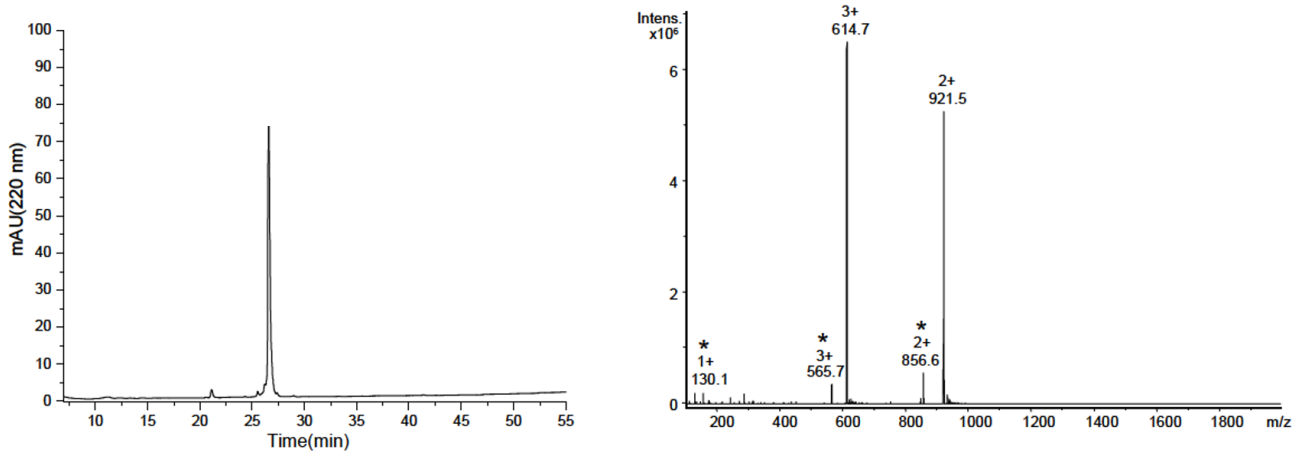


**Figure S1.** RP-HPLC profile and ESI-ion trap mass spectrum of GnRH-III–[$^{4}$Ser, $^{8}$Lys(Dau=Aoa)] (**K1**). ($MW_{cal}$ /$MW_{exp}$ = 1841.89/1841.05 g/mol, *fragment ion: amino sugar loss of Dau)

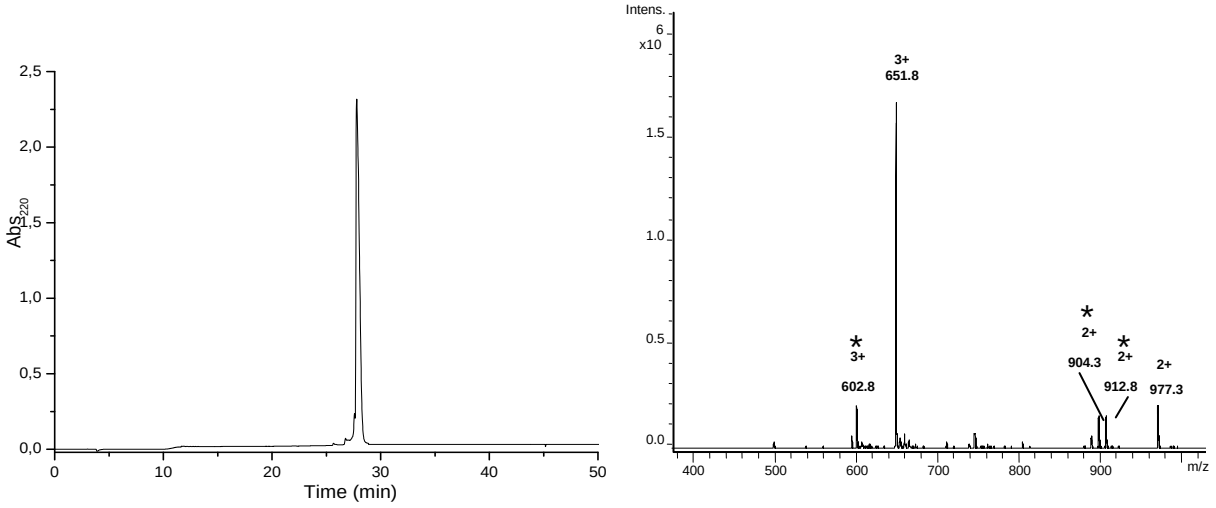


**Figure S2.** RP-HPLC profile and ESI-ion trap mass spectrum of GnRH-III–[$^{4}$Lys(Bu), $^{8}$Lys(Dau=Aoa)] (**K2**). ($MW_{cal}$ /$MW_{exp}$ = 1953.07/1952.70 g/mol).

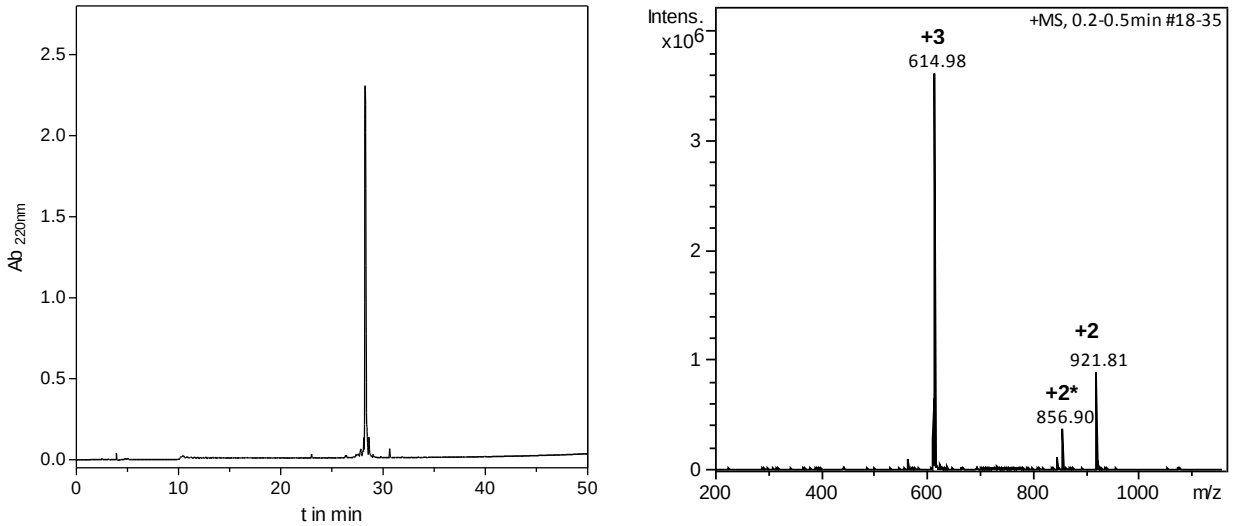


**Figure S3.** RP-HPLC profile and ESI-ion trap mass spectrum of GnRH-III–[$^{4}$Ser, $^{6}$D-Asp, $^{8}$Lys(Dau=Aoa)] (**1**) ($MW_{cal}$ /$MW_{exp}$ = 1841.89/1841.60 g/mol, *fragment ion: amino sugar loss of Dau)

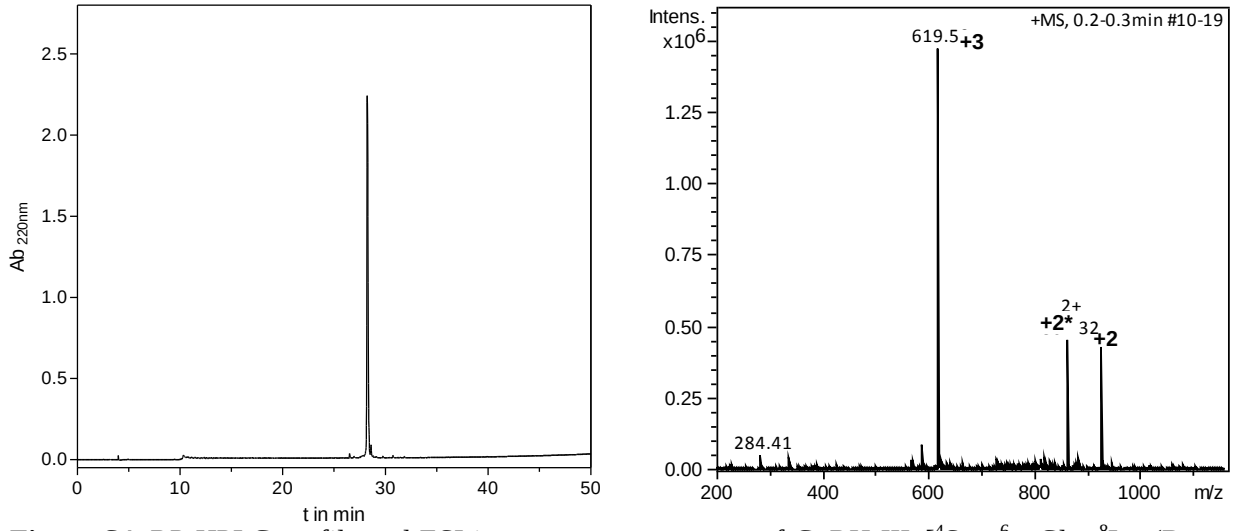


**Figure S4.** RP-HPLC profile and ESI-ion trap mass spectrum of GnRH-III–[$^{4}$Ser, $^{6}$D-Glu, $^{8}$Lys(Dau=Aoa)] (**2**) ($MW_{cal}$ /$MW_{exp}$ = 1855.91/1855.70 g/mol)

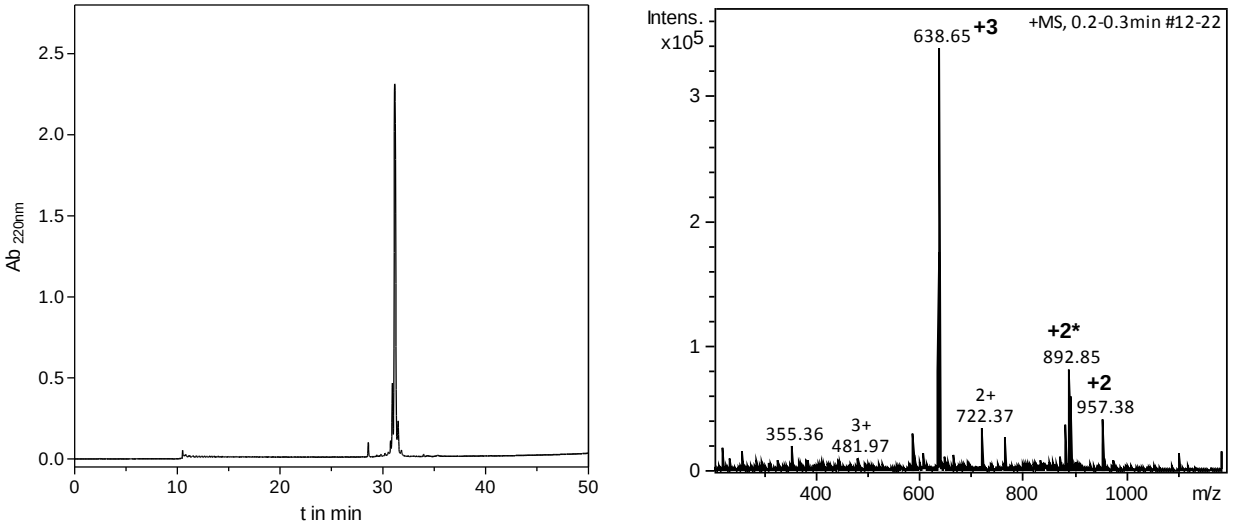


**Figure S5.** RP-HPLC profile and ESI-ion trap mass spectrum of GnRH-III–[$^{4}$Ser, $^{6}$D-Trp, $^{8}$Lys(Dau=Aoa)] (**3**) ($MW_{cal}$ /$MW_{exp}$ = 1913.01/1912.80 g/mol)

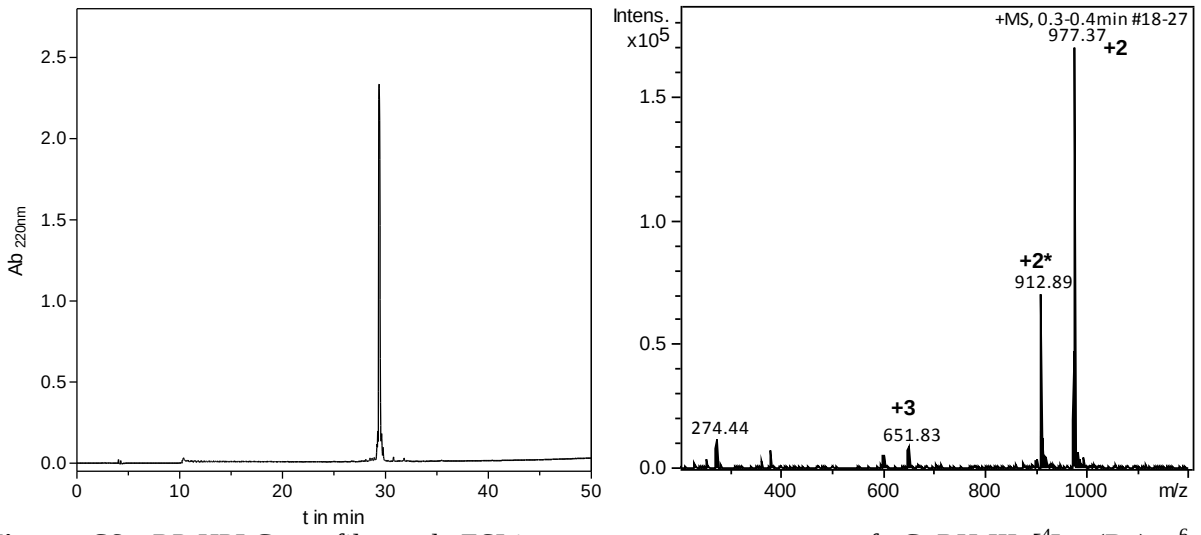


**Figure S6.** RP-HPLC profile and ESI-ion trap mass spectrum of GnRH-III–[$^{4}$Lys(Bu), $^{6}$D-Asp, $^{8}$Lys(Dau=Aoa)] (**4**) ($MW_{cal}$ /$MW_{exp}$ = 1953.07/1952.90 g/mol)

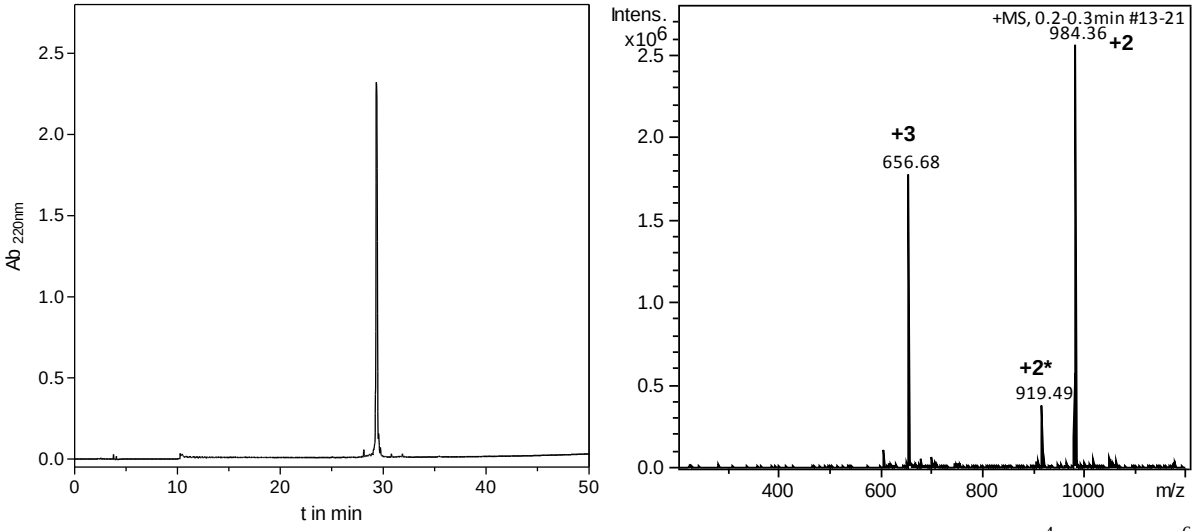


**Figure S7.** RP-HPLC profile and ESI-ion trap mass spectrum of GnRH-III–[$^{4}$Lys(Bu), $^{6}$D-Glu, $^{8}$Lys(Dau=Aoa)] (**5**) ($MW_{cal}$ /$MW_{exp}$ = 1966.93/1966.70 g/mol)

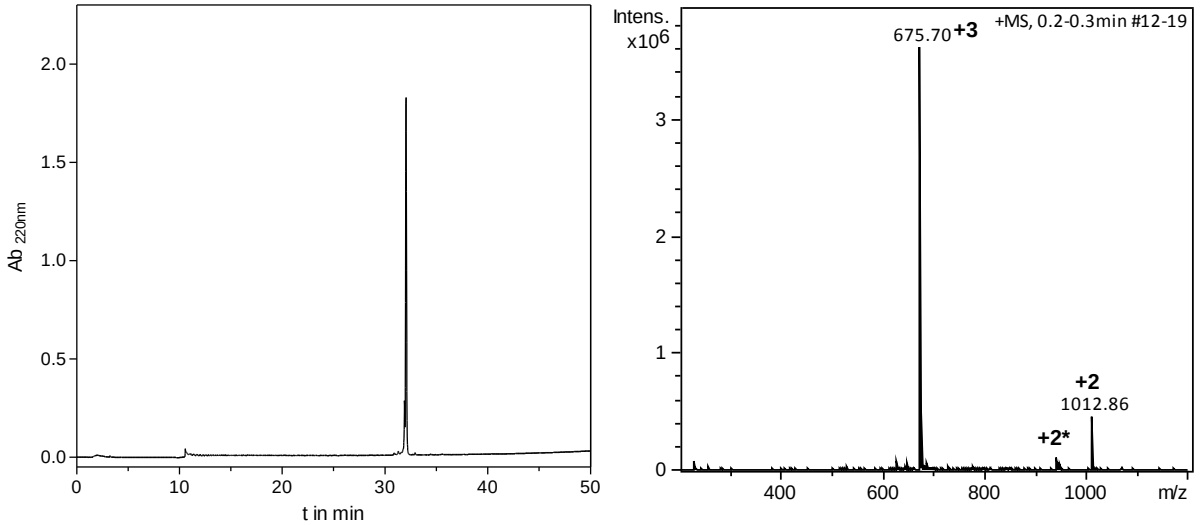


**Figure S8.** RP-HPLC profile and ESI-ion trap mass spectrum of GnRH-III–[$^{4}$Lys(Bu), $^{6}$D-Trp, $^{8}$Lys(Dau=Aoa)] (**6**) ($MW_{cal}$ /$MW_{exp}$ = 2024.03/2023.70)

**Table S1**. Fragments produced by the cleavage of GnRH-III-[$^{4}$Lys(Bu)/$^{4}$Ser, $^{6}$Aaa, $^{8}$Lys(Dau=Aoa)] bioconjugates in the presence of rat liver homogenate

| Code | Compound | Fragment | $MW_{cal}/MW_{exp}$ |
|---|---|---|---|
| **K1** | [$^{8}$Lys(Dau=Aoa)] | <EHWSHDWK(Dau=Aoa)PG-$NH_2$ | 1841.89/1841.66 |
| | | <EHWSHDWK(Dau=Aoa)P-OH | 1785.82/1785.27 |
| | | <EHWSHDWK(Dau=Aoa)-OH | 1688.70/1688.69 |
| | | H-WSHDWK(Dau=Aoa)-OH | 1440.49/1439.78 |
| | | H-HDWK(Dau=Aoa)PG-$NH_2$ | 1320.36/139.83 |
| | | H-HDWK(Dau=Aoa)-OH | 1167.18/1166.87 |
| | | H-K(Dau=Aoa)PG-$NH_2$ | 881.94/881.39 |
| | | H-K(Dau=Aoa)P-OH | 825.86/825.35 |
| | | H-K(Dau=Aoa)-OH | 728.75/728.34 |
| | | <EHWSH-OH | 676.68/676.23 |
| | | <EHWS-OH | 539.54/539.32 |
| | | <EHW-OH | 452.46/452.32 |
| | | H-DW-OH | 319.12/319.28 |
| **1** | [$^{6}$D-Asp, $^{8}$Lys(Dau=Aoa)] | <EHWSHdWK(Dau=Aoa)PG-$NH_2$ | 1841.89/1841.63 |
| | | <EHWSHdWK(Dau=Aoa)P-OH | 1785.82/1785.63 |
| | | <EHWSHdWK(Dau=Aoa)-OH | 1688.70/1688.44 |
| | | H-WSHdWK(Dau=Aoa)PG-$NH_2$ | 1593.65/1593.61 |
| | | H-WSHdWK(Dau=Aoa)-OH | 1440.49/1440.45 |
| | | H-SHdWK(Dau=Aoa)-OH | 1254.26/1253.83 |
| **2** | [$^{6}$D-Glu, $^{8}$Lys(Dau=Aoa)] | <EHWSHeWK(Dau=Aoa)PG-$NH_2$ | 1855.90/1855.67 |
| | | <EHWSHeWK(Dau=Aoa)P-OH | 1799.87/1799.79 |
| | | <EHWSHeWK(Dau=Aoa)-OH | 1702.76/1701.85 |
| | | H-WSHeWK(Dau=Aoa)PG-$NH_2$ | 1607.70/1607.63 |
| | | H-WSHeWK(Dau=Aoa)-OH | 1454.51/1453.91 |
| | | H-SHeWK(Dau=Aoa)-OH | 1268.30/1267.75 |
| | | H-K(Dau=Aoa)-OH | 728.75/728.33 |
| **3** | [$^{6}$D-Trp, $^{8}$Lys(Dau=Aoa)] | <EHWSHwWK(Dau=Aoa)PG-$NH_2$ | 1913.04/1912.79 |
| | | <EHWSHwWK(Dau=Aoa)P-OH | 1856.941856.64 |
| | | <EHWSHwWK(Dau=Aoa)-OH | 1759.85/1759.61 |
| | | H-WSHwWK(Dau=Aoa)-OH | 1511.61/1511.58 |
| | | H-SHwWK(Dau=Aoa)PG-$NH_2$ | 1478.58/1477.79 |
| | | H-SHwWK(Dau=Aoa)-OH | 1325.40/1324.04 |
| | | H-wWK(Dau=Aoa)-OH | 1101.18/1101.01 |
| | | H-K(Dau=Aoa)-OH | 728.75/728.34 |
| | | <EHWSHwW-OH | 1049.12/1049.06 |
| **K2** | [$^{4}$Lys(Bu), $^{8}$Lys(Dau=Aoa)] | <EHWK(Bu)HDWK(Dau=Aoa)PG-$NH_2$ | 1953.07/1952.79 |
| | | <EHWK(Bu)HDWK(Dau=Aoa)-OH | 1799.92/1799.69 |
| | | H-HDWK(Dau=Aoa)PG-$NH_2$ | 1320.36/1319.95 |
| | | H-HDWK(Dau=Aoa)-OH | 1167.18/1166.91 |
| | | H-K(Dau=Aoa)PG-$NH_2$ | 881.94/881.44 |
| | | H-K(Dau=Aoa)P-OH | 825.86/825.40 |
| | | H-K(Dau=Aoa)-OH | 728.75/728.37 |
| | | <EHWK(Bu)HD-OH | 902.96/902.84 |
| | | <EHWK(Bu)-OH | 650.73/650.71 |
| | | <EHW-OH | 452.46/452.31 |
| | | H-DW-OH | 319.32/319.27 |
| **4** | [$^{4}$Lys(Bu), $^{6}$D-Asp, $^{8}$Lys(Dau=Aoa)] | <EHWK(Bu)HdWK(Dau=Aoa)PG-$NH_2$ | 1953.07/1952.79 |
| | | <EHWK(Bu)HdWK(Dau=Aoa)P-OH | 1897.03/1896.90 |
| | | <EHWK(Bu)HdWK(Dau=Aoa)-OH | 1799.92/1799.81 |
| | | H-WK(Bu)HdWK(Dau=Aoa)-OH | 1551.67/1551.59 |
| | | H-K(Bu)HdWK(Dau=Aoa)PG-$NH_2$ | 1518.65/1517.88 |
| | | H-K(Bu)HdWK(Dau=Aoa)-OH | 1365.46/1364.92 |
| | | H-HdWK(Dau=Aoa)-OH | 1167.18/1166.90 |
| | | <EHWK(Bu)-OH | 650.73/650.43 |
| | | <EHW-OH | 452.46/452.3 |
| **5** | [$^{4}$Lys(Bu), $^{6}$D-Glu, $^{8}$Lys(Dau=Aoa)] | <EHWK(Bu)HeWK(Dau=Aoa)PG-$NH_2$ | 1967.13/1966.82 |
| | | <EHWK(Bu)HeWK(Dau=Aoa)P-OH | 1911.06/1910.81 |
| | | <EHWK(Bu)HeWK(Dau=Aoa)-OH | 1813.94/1813.70 |

| | | | |
|---|---|---|---|
| | | H-WK(Bu)HeWK(Dau=Aoa)-OH | 1565.70/1565.13 |
| | | H-HeWK(Dau=Aoa)-OH | 1181.22/1180.67 |
| **5** | [$^{4}$Lys(Bu), $^{6}$D-Glu, $^{8}$Lys(Dau=Aoa)] | H-K(Bu)HeWK(Dau=Aoa)-OH | 1379.49/1378.93 |
| | | <EHW-OH | 452.46/452.31 |
| **6** | [$^{4}$Lys(Bu), $^{6}$D-Trp, $^{8}$Lys(Dau=Aoa)] | <EHWK(Bu)HwWK(Dau=Aoa)PG-$NH_2$ | 2024.22/2024.25 |
| | | <EHWK(Bu)HwWK(Dau=Aoa)P-OH | 1968.16/1967.84 |
| | | <EHWK(Bu)HwWK(Dau=Aoa)-OH | 1871.04/1870.50 |
| | | <EHWK(Bu)HwW-OH | 1160.30/1160.21 |
| | | H-K(Bu)HwWK(Dau=Aoa)-OH | 1436.59/1436.24 |
| | | H-HwWK(Dau=Aoa)-OH | 1238.32/1232.04 |
| | | H-K(Dau=Aoa)-OH | 728.75/728.33 |
| | | <EHWK(Bu)-OH | 650.73/650.43 |
| | | H-HwW-OH | 527.58/527.37 |

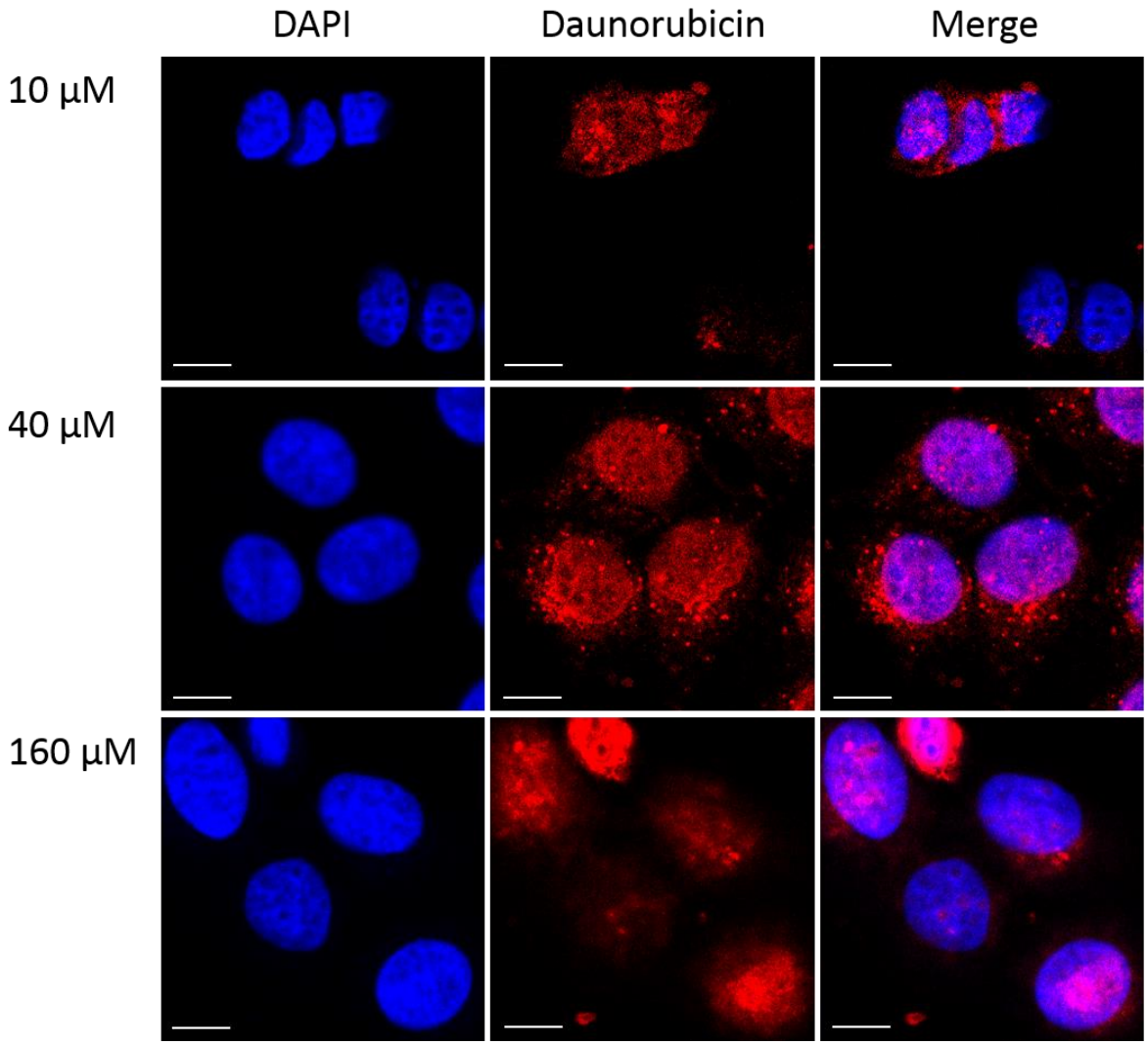


**Figure S9**. Cellular uptake of bioconjugate **K1** (10 µM, 40 µM and 160 µM) visualized by confocal laser scanning microscopy (CLSM) (scale bars represent 10 µm).

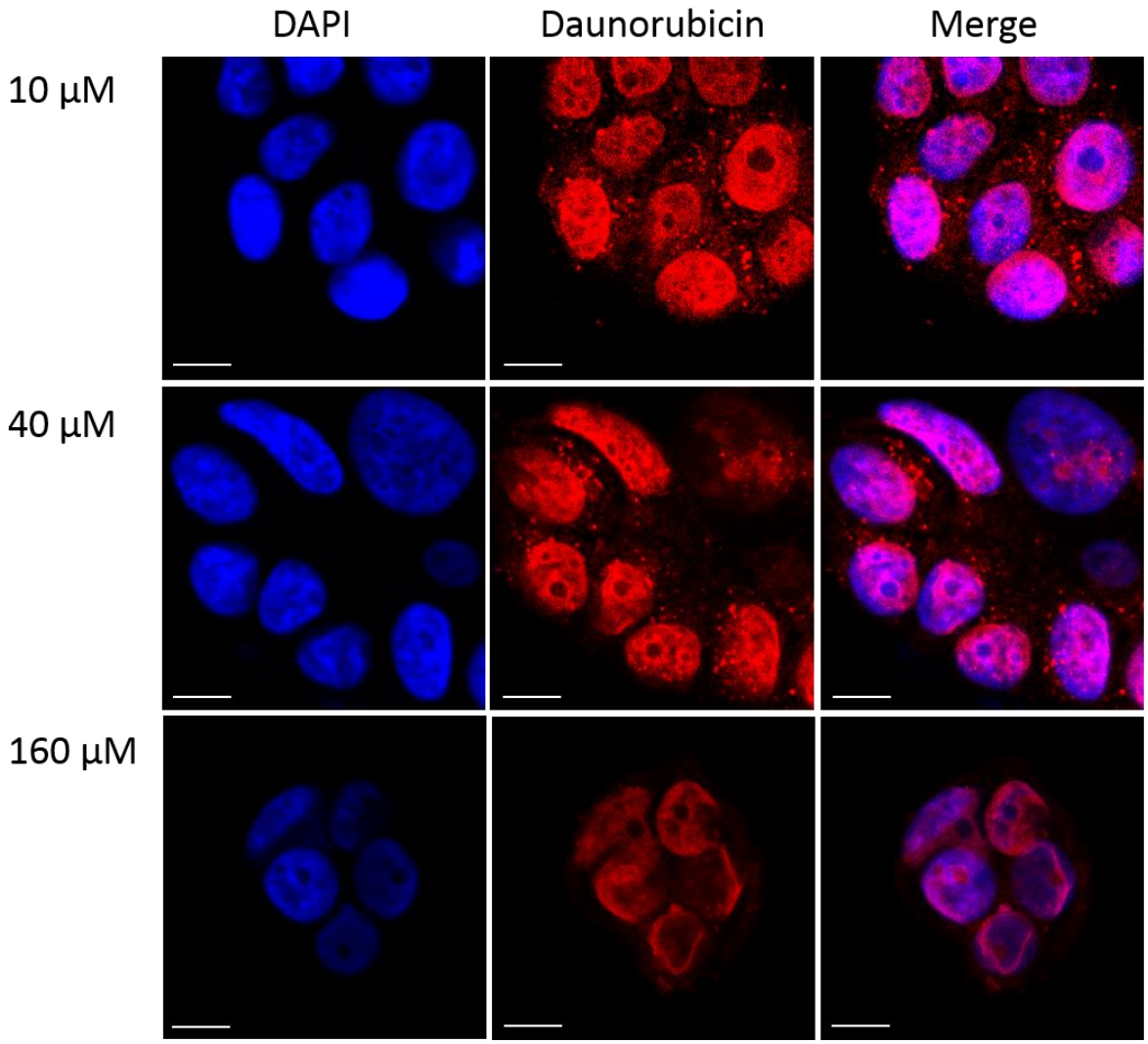


**Figure S10**. Cellular uptake of bioconjugate **1** (10 µM, 40 µM and 160 µM) visualized by confocal laser scanning microscopy (CLSM) (scale bars represent 10 µm).

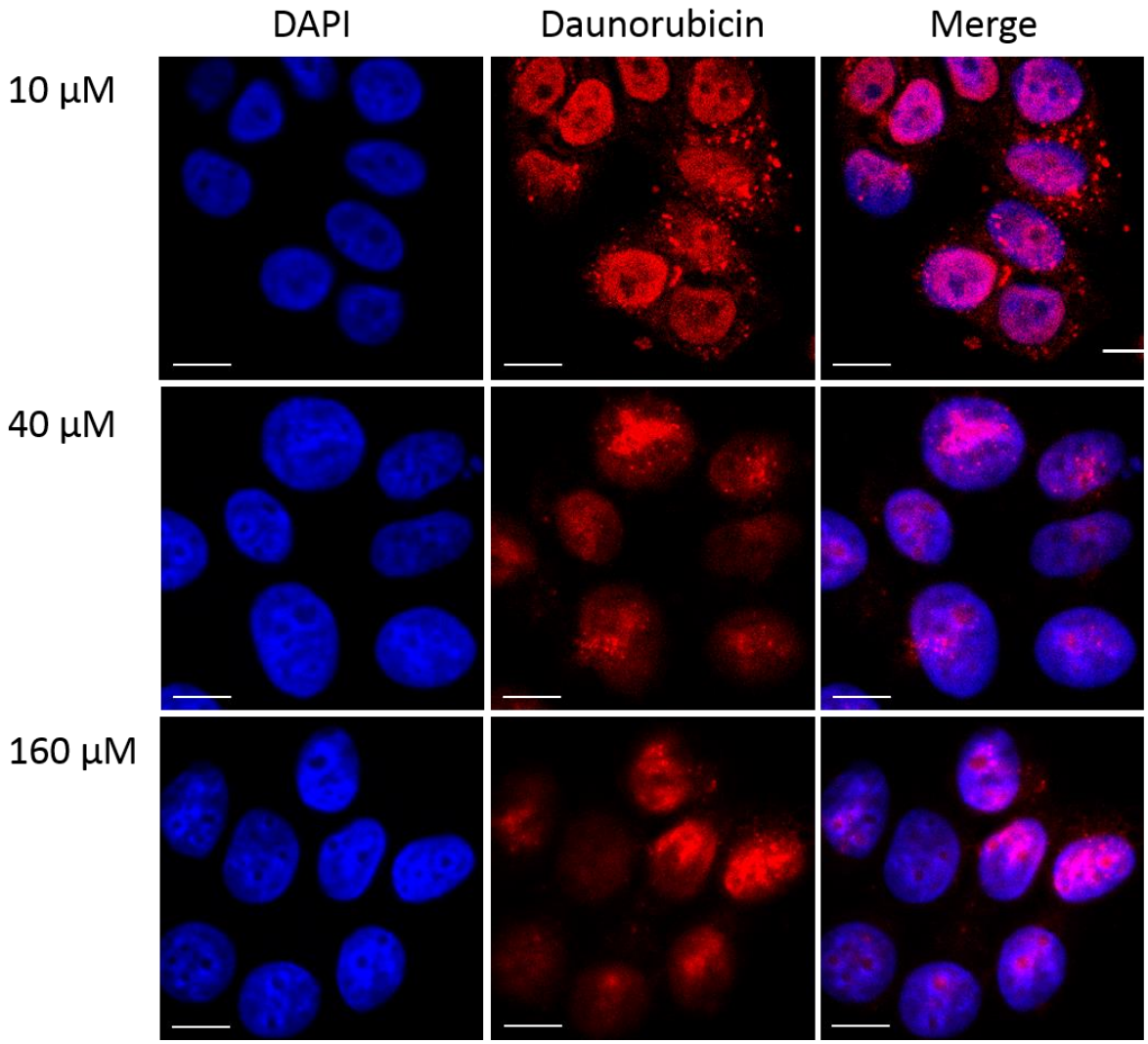


**Figure S11.** Cellular uptake of bioconjugate **2** (10 µM, 40 µM and 160 µM) visualized by confocal laser scanning microscopy (CLSM) (scale bars represent 10 µm).

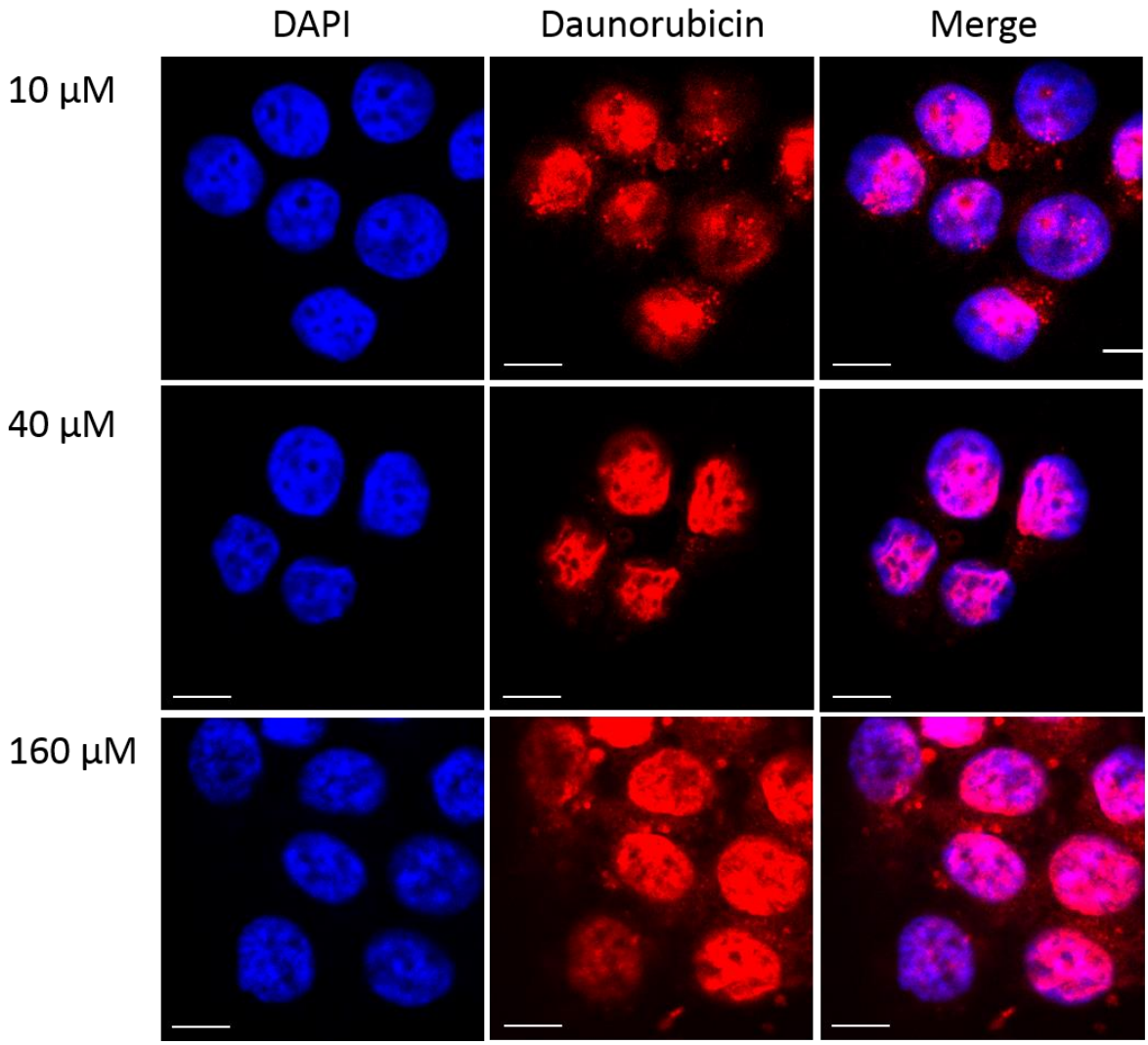


**Figure S12.** Cellular uptake of bioconjugate **K2** (10 µM, 40 µM and 160 µM) visualized by confocal laser scanning microscopy (CLSM) (scale bars represent 10 µm).

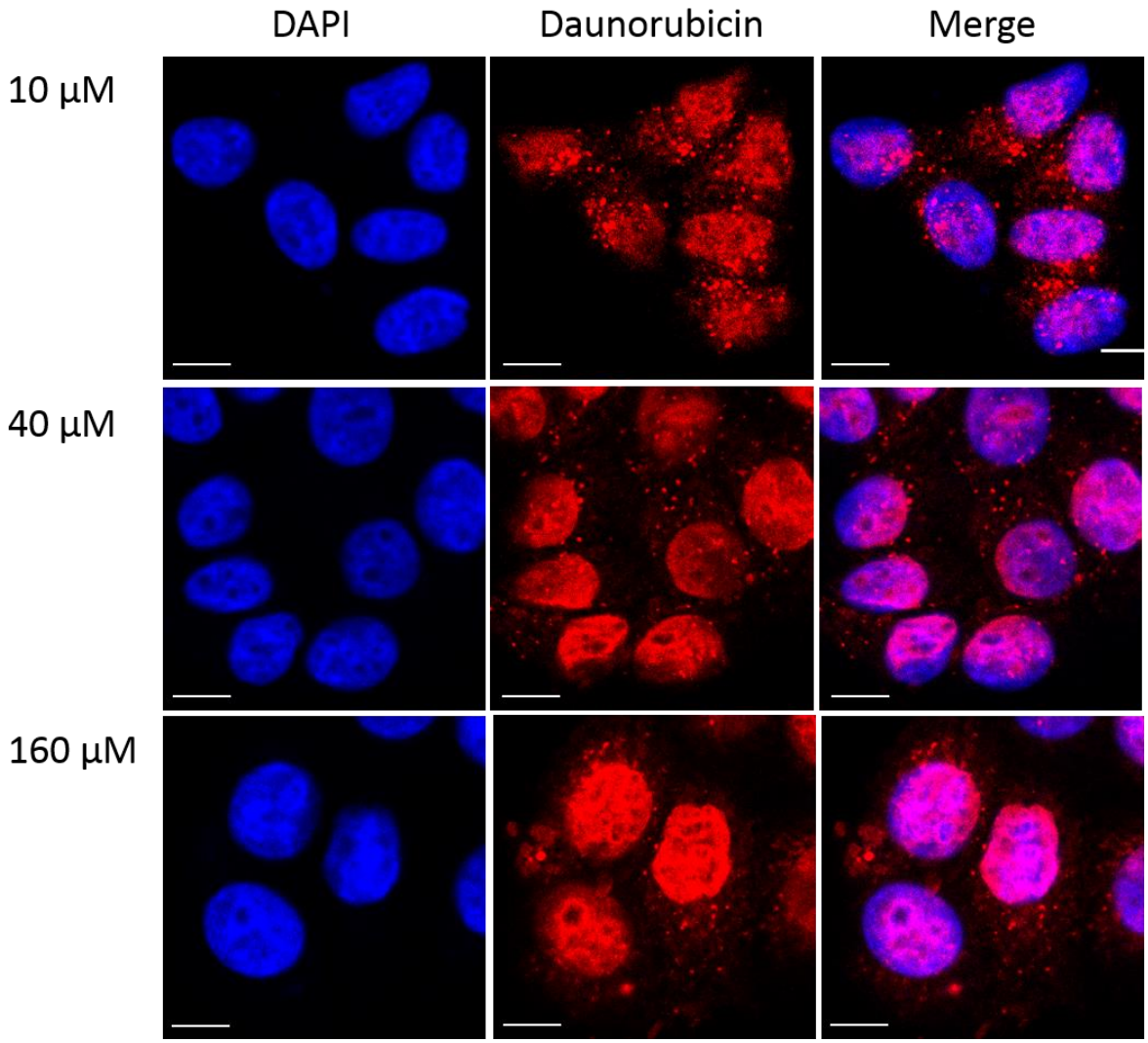


**Figure S13.** Cellular uptake of bioconjugate **4** (10 µM, 40 µM and 160 µM) visualized by confocal laser scanning microscopy (CLSM) (scale bars represent 10 µm).

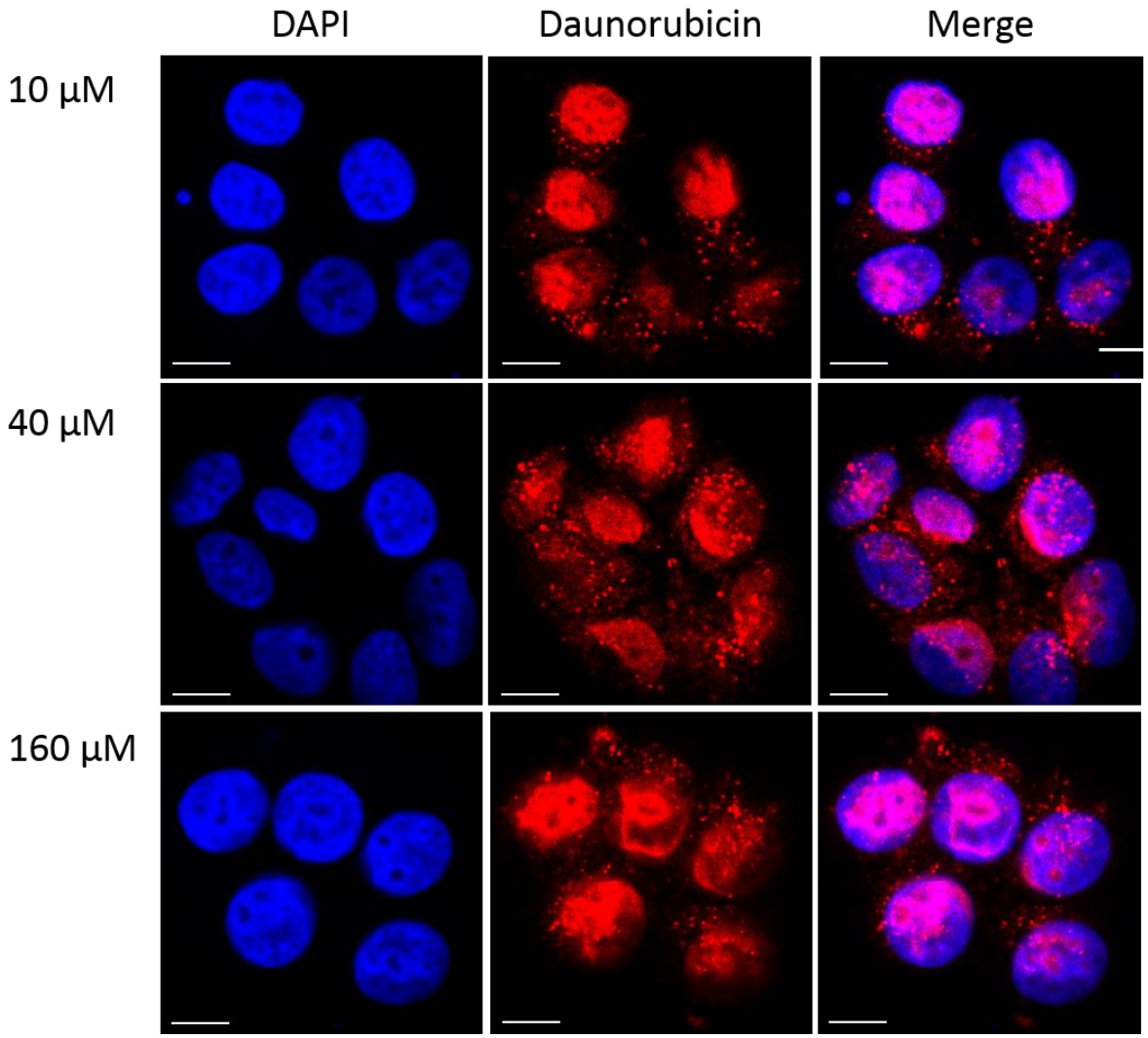


**Figure S14.** Cellular uptake of bioconjugate **5** (10 µM, 40 µM and 160 µM) visualized by confocal laser scanning microscopy (CLSM) (scale bars represent 10 µm).

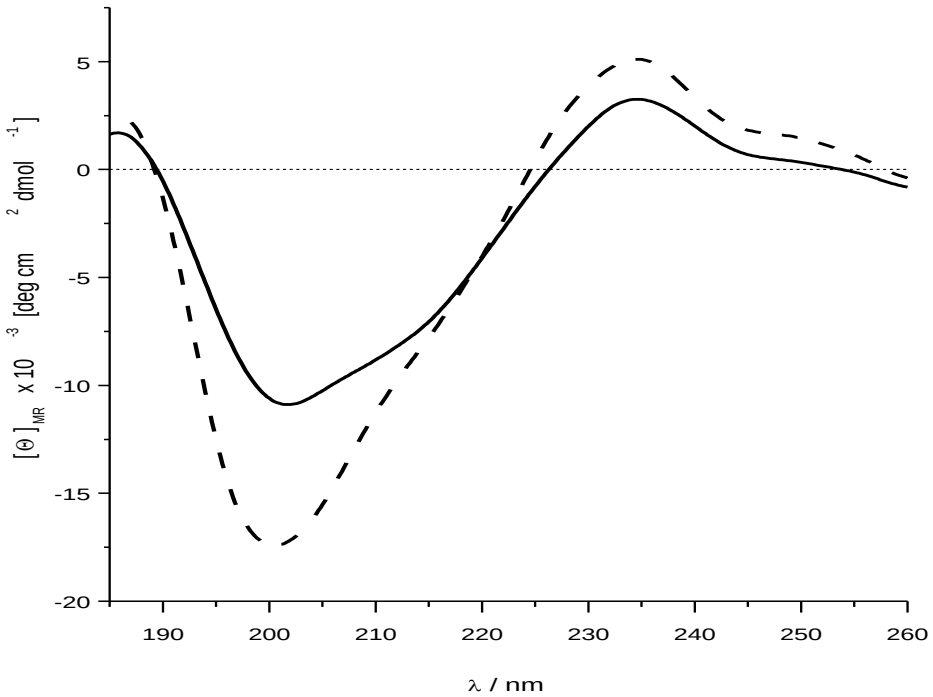


**Figure S15.** Far-UV ECD spectra of **K1** (dash) and **1** (solid) in water.

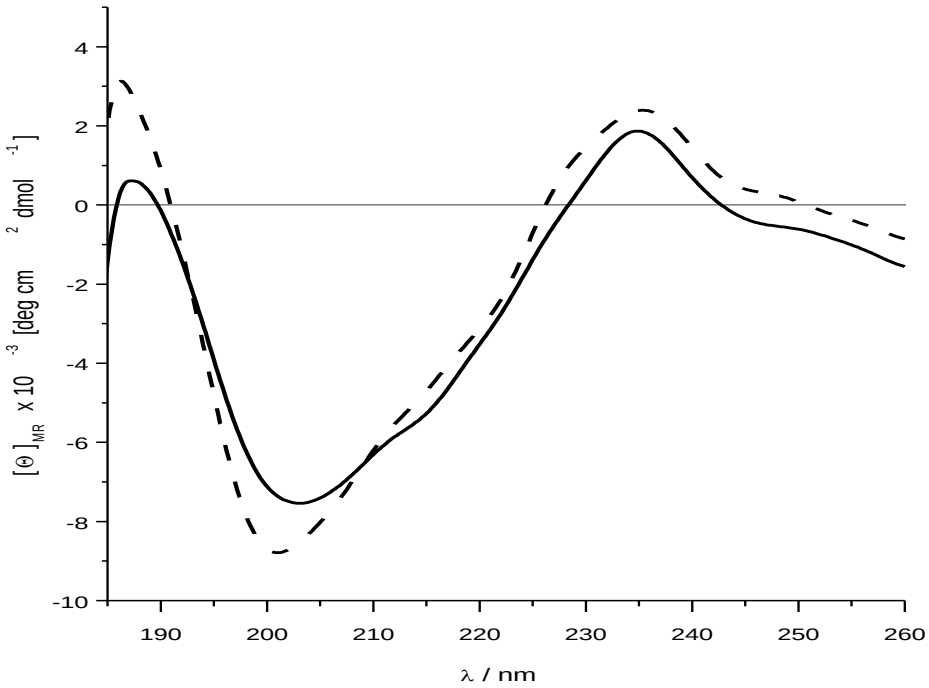


**Figure S16.** Far-UV ECD spectra of **K2** (dash) and **4** (solid) in water.